PHYSICAL REVIEW C VOLUME 12, NUMBER 5 NOVEMBER 1975

Spin-dependent potentials for deuteron-nucleus scattering*

L. D. Knutson† and W. Haeberli
University of Wisconsin, Madison, Wisconsin 53706
(Received 7 July 1975)

Measurements of the cross section, the vector analyzing power, and the three tensor analyzing powers for deuteron elastic scattering from ^{90}Zr at 5.5 MeV and from ^{208}Pb at 9.0 MeV are presented. These measurements and additional measurements obtained from the literature are analyzed in terms of the optical model. The folding model is used to calculate the spin-dependent potentials from the known nucleon-nucleus potentials, and the central terms in the optical potential are determined empirically. Acceptable agreement is obtained for the cross section and vector analyzing power. The calculations reproduce the observed tensor analyzing powers for sub-Coulomb energies but not for energies above the Coulomb barrier.

NUCLEAR REACTIONS ^{90}Zr($\vec{d}$,d), E_d=5.5 MeV; ^{208}Pb($\vec{d}$,d), E_d=9.0 MeV; measured polarization parameters iT_{11}, T_{20}, T_{21}, $T_{22}(E_d,\theta)$; cross sections $\sigma(E_d,\theta)$. Enriched targets, optical model analysis.

I. INTRODUCTION

In this paper we present measurements of the cross section and analyzing powers[1] for deuteron elastic scattering from ^{90}Zr and ^{208}Pb at energies below the Coulomb barrier. These measurements, and additional measurements at higher energies obtained from the literature, are subjected to an optical model analysis in which the spin dependent terms in the potential are calculated from the folding model.[2] In this model, one assumes that the deuteron-nucleus potential is equal to the sum of the neutron-nucleus and proton-nucleus potentials averaged over the internal motion of the deuteron.

It has previously been shown that calculations using the folding model central potentials do not satisfactorily reproduce the measured differential cross sections.[3,4] In order to obtain good agreement it is necessary to change the strength of the real central potential by 10–20% and to increase the strength of the imaginary potential.[3] A 10–20% change in the strength of the central potential produces large changes in the calculated cross section and analyzing powers. Consequently, the usefulness of the folding model is limited. However, the model may still be useful to predict the spin dependent parts of the potential and thus to reduce ambiguities in the optical model analysis which result from the large number of parameters. Less accuracy is required for the spin dependent terms, since they are relatively weak compared to the central potential. Our purpose here is to determine whether the spin-orbit and tensor potentials predicted by the folding model are quantitatively consistent with the observed vector and tensor analyzing powers for deuteron elastic scattering.

In Sec. II the experimental apparatus and the analyzing power measurements will be described. In Sec. III we will discuss the predicted spin dependence of the Coulomb part of the deuteron-nucleus potential. The calculation of the nuclear part of the potential will be described in Sec. IV. The optical model calculations will be presented in Secs. V and VI. Some of the results to be discussed here have previously been reported elsewhere.[5]

II. MEASUREMENTS

Angular distributions of the differential cross section, the vector analyzing power (iT_{11}), and the three tensor analyzing powers (T_{20}, T_{21}, and T_{22}) have been measured for deuteron elastic scattering from ^{90}Zr at 5.5 MeV and from ^{208}Pb at 9.0 MeV. The measurements were carried out using the deuteron beam from the University of Wisconsin Lamb-shift polarized ion source.[6] The analyzing powers presented here are defined according to the Madison Convention[7]; a more detailed discussion of these quantities can be found in Ref. 1.

The measurements were carried out as follows. A beam of polarized deuterons was incident on a self-supporting target made from isotopically enriched material (98.1% for ^{90}Zr and 99.5% for ^{208}Pb). The targets were approximately 1 mg/cm^2 thick. Scattered deuterons and reaction products were detected by counter telescopes located to one side of the beam. Four telescopes were used to measure the analyzing powers at four angles simultaneously. The detected particles were identified by an on-line computer program[8] which makes use of the particle identification technique of Hird and Ollerhead.[9] The measurements were corrected for the electronic dead time of the counting system using the technique described in Ref. 10. The fractional dead time was less than 1% in all cases.

Beam integration was accomplished by counting the number of deuterons scattered into two monitor detectors located symmetrically to the left and right of the beam at 13.1°. The counting rate for the monitor detectors is independent of the polarization state of the beam, since the analyzing powers are essentially zero at far forward angles according to optical model calculations. Thus

III. SPIN DEPENDENCE IN COULOMB SCATTERING

In this section we consider the elastic scattering of deuterons by a pure Coulomb field. It will be shown that the Coulomb potential energy contains a spin dependent term if the deuteron D state is taken into account. The analyzing powers which arise from this Coulomb interaction will be calculated and the results compared with the observed analyzing powers for sub-Coulomb scattering.

Consider the potential energy $V_c(\vec{r})$ of a deuteron whose c.m. is at position $\vec{r}$ with respect to a point charge Ze. Since the Coulomb force acts only on to the second derivative of the electrostatic potential, as one would expect from the above discussion.

The effect of the Coulomb tensor potential on the analyzing powers for elastic scattering is small because the potential is weak. Using the measured value of the deuteron quadrupole moment,[14] we find that the tensor potential is only 0.4% of the central Coulomb potential at a radius of 10 fm. Although the tensor potential is weak, it extends to rather large radii since it falls off as r^{-3}, whereas the nuclear forces fall off exponentially outside the nucleus. Thus, for energies sufficiently far below the Coulomb barrier, the analyzing powers for deuteron elastic scattering should arise primarily from the Coulomb potential.

The effect of the Coulomb tensor potential on the deuteron scattering process was calculated using the distorted-wave Born approximation for elastic scattering. The method employed is similar to a method developed by Kim and Thomas.[15] The distorting potential was taken to be Ze^2/r, so that the distorted waves are just the Coulomb wave functions. The Coulomb tensor potential was treated as a perturbation. When this approximation is used one obtains a closed form expression for the cross section and the analyzing powers. The details of this calculation can be found in Ref. 12. The calculated values of iT_{11} and T_{20} for ^{208}Pb at 9 MeV are compared with the measurements in Fig. 1. One notes that for T_{20} the calculations are roughly a factor of 2 or 3 smaller in magnitude than the measurements, although the sign and shape of the analyzing powers are correctly predicted. Similar results were obtained for T_{21} and T_{22}. The disagreement between the calculations and the measurements is even more pronounced for iT_{11}. The magnitude of the measured vector analyzing power is typically 0.005, whereas the calculated values are zero. It appears that the nuclear spin dependent forces have a significant influence on the measurements.

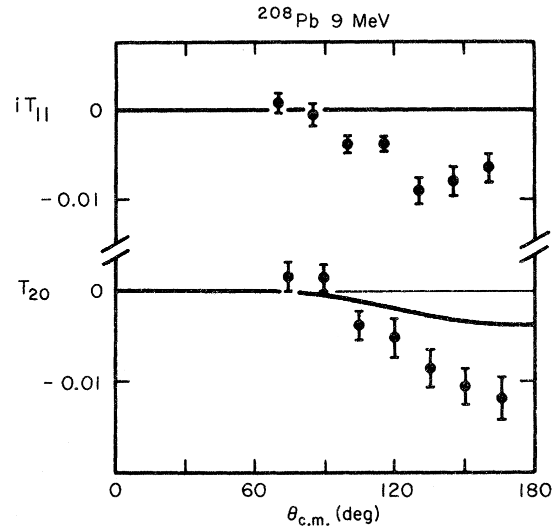

FIG. 1. Angular distributions of the analyzing powers iT_{11} and T_{20} for deuteron elastic scattering from ^{208}Pb at 9 MeV. The curves show the calculated analyzing powers for the potential given in Eq. (2), which includes Coulomb interactions only. The calculated values of iT_{11} are zero.

IV. FOLDING MODEL POTENTIALS

In this section we discuss the nuclear spin dependent potentials predicted by the folding model. In this model the deuteron-nucleus potential is given by[2]

$$\langle m|V(\vec{r})|m'\rangle = \langle \phi_d^m|[V_n(\vec{r}-\tfrac{1}{2}\vec{\rho}) + V_p(\vec{r}+\tfrac{1}{2}\vec{\rho})]|\phi_d^{m'}\rangle , \quad (4)$$

where V_n and V_p are the neutron-nucleus and proton-nucleus potentials, respectively. If the nucleon-nucleus potentials in Eq. (4) consist of central and spin-orbit terms, the deuteron potential will likewise contain a central and a spin-orbit term.[2] If the deuteron D state is included in the calculation, the deuteron potential will in addition contain a tensor potential of the form[16]

$$V_T(\vec{r}) = F(r)T_r , \quad (5)$$

where T_r is defined in Eq. (3).

The folding model potentials were calculated from Eq. (4) using the method of Raynal.[13] The potentials V_n and V_p were obtained from the analysis of Becchetti and Greenlees,[17] and the deuteron wave function was taken to be that derived from the nucleon-nucleon potential of Hamada and Johnston.[18]

The calculated spin dependent potentials for ^{90}Zr are shown in Fig. 2. The tensor potential is complex because the nucleon-nucleus central potential, from which it arises, is complex. The folding model spin-orbit potential is purely real since it arises from the nucleon-nucleus spin-orbit potentials which are assumed to be real at these energies. The potentials for ^{208}Pb are similar, but are slightly smaller in magnitude and extend to a larger radius than the ^{90}Zr potentials.

A. Tensor potential

As discussed in Sec. III, the tensor potential arises because the deuteron is not spherically symmetric. The real part of the tensor potential shown in Fig. 2 has a qualitative resemblance to the second derivative of the nucleon-nucleus central potential (see

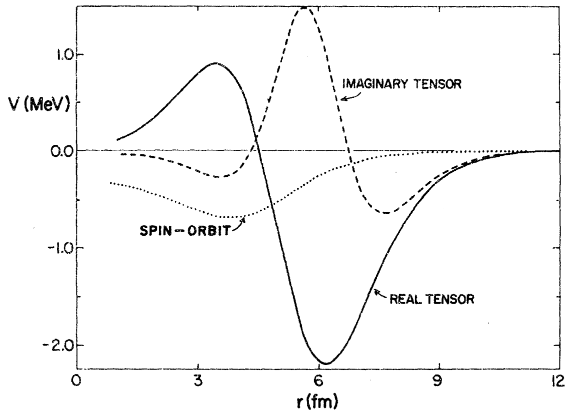

FIG. 2. Spin dependent parts of the folding model potential for ^{90}Zr as a function of the deuteron-nucleus separation. The real and imaginary parts of $F(r)$ [see Eq. (5)] are given by the solid and dashed curves, respectively. The spin-orbit potential is obtained by multiplying the dotted curve by $\vec{l}\cdot\vec{s}$.

Ref. 4) as one would expect from the argument in

duces the folding model potential are listed in Table I. In Fig. 3, the exact folding model potential for ^{90}Zr (solid curve) is compared with the potential calculated from Eq. (6) using the parameters listed in Table I (dotted curve). It would appear that for most purposes the exact potential and the analytic representation can be used interchangeably.

It is interesting to compare the folding model spin-orbit potential with the spin-orbit potentials which have been used in previous phenomenological optical model analyses (see, for example, Ref. 25 and references cited therein). Typical values of the parameters which describe the phenomenological spin-orbit potential are

$$V_{so} = 7 \text{ MeV}, \quad r_{so} = 0.8 \text{ fm}, \quad a_{so} = 0.5 \text{ fm}. \qquad (8)$$

The primary difference between the potential given in Eq. (8) and those listed in Table I is that the diffuseness parameter is larger for the folding model potential. Note that the analytic expression for the spin-orbit potential contains a factor $1/a_{so}$, and consequently the folding model potential is smaller in magnitude at its peak than the phenomenological potential. In Fig. 3 we compare the spin-orbit

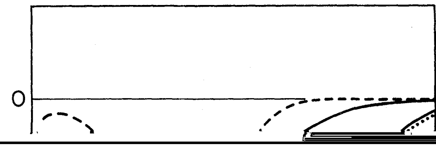

power (see Sec. VI).

The six parameters describing the nuclear central potentials were adjusted to obtain a good fit to the measured cross sections and vector analyzing powers. The final parameters are listed in

TABLE II. Optical model parameters determined by fitting the cross section and vector analyzing power measurements. The column labeled "spin-orbit" indicates whether the spin-

The dashed curves in Fig. 5 show the analyzing powers which result when the folding model tensor terms are included in the potential and the analyz-

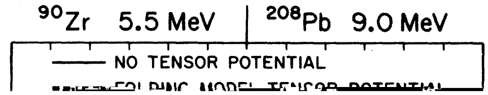

and approximate magnitude of all three tensor analyzing powers for both target nuclei without the use of adjustable parameters.

potential has no simple physical basis.

When the folding model tensor potential was included in the analysis, the resulting optical model calculations successfully reproduced the measured

VII. SUMMARY AND CONCLUSIONS

For the targets and energies considered here, the optical model calculations which make use of the folding model spin-orbit potential provide reasonable agreement with measurements of the vector analyzing power. For energies above the Coulomb barrier, the fits are comparable in quality to those obtained in calculations which use more standard spin-orbit potentials. We conclude that the measurements discussed here show no clear preference for either the folding model potential or for the standard phenomenological potential. In future analyses, it would be interesting to compare the two spin-orbit potentials over a wider range of targets and energies. If it should turn out that the two potentials consistently provide comparable fits, one would naturally prefer the folding model potential, since it is derived from a physical model of the interaction whereas the standard spin-orbit

tensor analyzing powers for sub-Coulomb scattering. However, a similar calculation for deuteron scattering from ^{90}Zr at 10 MeV was unsuccessful. In view of the mixed success of these results, it is not possible to draw firm conclusions concerning the accuracy of the folding model tensor potentials. The lack of agreement in the latter analysis is not necessarily the result of using an incorrect tensor potential, but could also result from the use of inaccurate central potentials. Alternatively, the deterioration of the fits with increasing energy may be an indication that the folding model potential is correct outside the nucleus but inaccurate in the nuclear interior. The resolution of these questions will require more detailed optical model analyses.

The authors are indebted to J. M. Lohr and R. P. Goddard for allowing us to make use of their analyzing power measurements prior to publication.

---

*Work supported in part by the U. S. Atomic Energy Commission.

† Present address: Nuclear Physics Laboratory, University of Washington, Seattle, Washington 98195.

[1]S. E. Darden, in *Polarization Phenomena in Nuclear Reactions*, edited by H. H. Barschall and W. Haeberli (Univ. of Wisconsin Press, Madison, 1971), p. 39.

[2]S. Watanabe, Nucl. Phys. 8, 484 (1958).

[3]F. G. Perey and G. R. Satchler, Nucl. Phys. A97, 515 (1967).

[4]P. W. Keaton, Jr., and D. D. Armstrong, Phys. Rev. C 8, 1692 (1973).

[5]L. D. Knutson and W. Haeberli, Phys. Rev. Lett. 30, 986 (1973).

[6]T. B. Clegg, G. A. Bissinger, W. Haeberli, and P. A. Quin, in *Polarization Phenomena in Nuclear Reactions* (see Ref. 1), p. 835.

[7]*Polarization Phenomena in Nuclear Reactions* (see Ref. 1), p. xxv.

[8]S. E. Vigdor and H. Liers, University of Wisconsin Internal Report OPIS71, 1971 (unpublished).

[9]B. Hird and R. W. Ollerhead, Nucl. Instrum. Methods

tory Report No. ANL–TRANS–258, 1965 (unpublished)].

[14]R. V. Reid, Jr., and M. L. Vaida, Phys. Rev. Lett. 29, 494 (1972).

[15]Y. N. Kim and H. C. Thomas, Phys. Rev. 148, 1083 (1966).

[16]G. R. Satchler, Nucl. Phys. 21, 116 (1960).

[17]F. D. Becchetti, Jr., and G. W. Greenlees, Phys. Rev. 182, 1190 (1969).

[18]T. Hamada and I. D. Johnston, Nucl. Phys. 34, 382 (1962).

[19]P. Schwandt and W. Haeberli, Nucl. Phys. A123, 401 (1969).

[20]A. Djaloeis and J. Nurzynski, Nucl. Phys. A163, 113 (1971).

[21]A. Djaloeis and J. Nurzynski, Nucl. Phys. A181, 280 (1972).

[22]G. Perrin *et al.*, Nucl. Phys. A206, 623 (1973).

[23]M. Irshad and B. A. Robson, Nucl. Phys. A218, 504 (1974).

[24]R. Roche, N. VanSen, G. Perrin, J. C. Gondrand, A. Fiore, and H. Müller, Nucl. Phys. A220, 381 (1974).

[29]R. P. Goddard (private communication).

[30]S. E. Vigdor, R. D. Rathmell, H. S. Liers, and W. Haeberli, Nucl. Phys. A210, 70 (1973).

[31]R. P. Goddard and W. Haeberli, Bull. Am. Phys. Soc. 18, 1393 (1973).

[32]D. J. Hooten and R. C. Johnson, Nucl. Phys. A175, 583 (1971).